Physics Letters B 795 (2019) 271–276

Contents lists available at ScienceDirect

Physics Letters B

www.elsevier.com/locate/physletb

Measurement of proton-evaporation rates in fusion reactions leading to transfermium nuclei

A. Lopez-Martens [a,*], A.V. Yeremin [b], M.S. Tezekbayeva [b,c], Z. Asfari [d], P. Brionnet [d,1], O. Dorvaux [d], B. Gall [d], K. Hauschild [a], D. Ackermann [e], L. Caceres [e], M.L. Chelnokov [b], V.I. Chepigin [b], M.V. Gustova [b], A.V. Isaev [b], A.V. Karpov [b], A.A. Kuznetsova [b], J. Piot [e], O.N. Malyshev [b], A.G. Popeko [b], Yu.A. Popov [b], K. Rezynkina [a,2], H. Savajols [e], A.I. Svirikhin [b], E.A. Sokol [b], P. Steinegger [b]

[a] CSNSM, IN2P3-CNRS, Université Paris Sud et Université Paris Saclay, Orsay, France
[b] FLNR, JINR, Dubna, Russia
[c] Institute of Nuclear Physics, Ministry of Energy of the Republic of Kazakhstan, Almaty, Republic of Kazakhstan
[d] IPHC, IN2P3-CNRS, Université de Strasbourg, Strasbourg, France
[e] GANIL, Caen, France

ARTICLE INFO

Article history:
Received 26 November 2018
Received in revised form 27 May 2019
Accepted 10 June 2019
Available online 11 June 2019
Editor: V. Metag

Keywords:
Fusion-evaporation reaction
Proton evaporation
Super heavy nuclei
Cross section

ABSTRACT

The analysis of fission events following the implantation of evaporation residues produced in the fusion reaction of ^{50}Ti and ^{209}Bi at different bombarding energies has revealed 5 millisecond decays, which are attributed to the spontaneous fission of proton-evaporation channels. The average cross sections for proton evaporation are found to be ∼100 and 10 times smaller than the largest neutron-evaporation channel cross section at the same excitation energy. These results suggest that the proton evaporation channel, albeit weak, may represent a realistic alternative to synthesize new, more neutron rich super heavy nuclei.

1. Introduction

The synthesis of new heavy isotopes addresses fundamental questions in nuclear physics, astrophysics and atomic physics: what is the extent of the nuclear chart and what are the properties of nuclei in extreme conditions of charge and mass ? Can superheavy nuclei be produced in the nucleosynthesis processes by which the heaviest stable or very long-lived elements on earth have been produced ? What is the atomic organisation of these very heavy nuclei ? In recent years, a very successful way of producing heavier and heavier nuclei has been the use of fusion-evaporation reactions using ^{48}Ca projectiles and actinide targets [1]. This research program has led to the discovery of the heaviest element with Z = 118 protons, oganesson. To go further in proton number, one can accelerate beams heavier than Ca and hopefully synthesise elements beyond oganesson. To go towards more neutron-rich nuclei, closer to the predicted "Island of Stability" [2], target materials such as ^{251}Cf and ^{254}Es can be envisaged, though the procurement of such enriched targets in sufficient quantities is not an easy task. Another route would be to produce new more neutron-rich isotopes via 1-proton and x neutron-evaporation reactions (pxn), for which transmission efficiencies into recoil separators are more or less the same as for the neutron-evaporation (xn) channels (in contrast to the αxn channel which suffers from a large reduction in transmission). As an example, one could imagine synthesizing moscovium (Mc, Z = 115) nuclei with the standard ^{48}Ca beam and a ^{248}Cm target instead of ^{243}Am. This would yield Mc isotopes at least 4 neutrons richer than what has been achieved up to now. The investigation of p-evaporation channels is therefore an important direction to pursue in terms of the continued effort to map the uncharted areas of the Segré chart but also in terms of understanding the reaction mechanisms that lead to the formation of the heaviest nuclei. Further-

* Corresponding author.
E-mail address: Araceli.Lopez-Martens@csnsm.in2p3.fr (A. Lopez-Martens).
[1] Current address: RIKEN, Wako, Japan.
[2] Current address: IPHC, IN2P3-CNRS, Université de Strasbourg, Strasbourg, France.

https://doi.org/10.1016/j.physletb.2019.06.010

more, quantifying the relative cross section for charged-particle emission with respect to neutron evaporation from such heavily-charged systems is necessary in view of the fact that all Z and A assignments of the heaviest known nuclei have been made assuming that the super heavy compound-nucleus formation is followed exclusively by neutron emission.

There are reports of very early investigations on pxn reactions leading to ^{256}Md using light ions [3], and on pxn and αxn evaporation channels in ^{208}Pb + $^{48-50}$Ti reactions [4], in which the upper limits of the (Ti, pxn) or (Ti, αxn) reaction cross sections were determined to be at a level of about one hundredth of the (Ti,xn) reaction cross section. In experiments with SHIP at GSI where the evaporation residues from reactions of ^{50}Ti on ^{209}Bi were investigated for the first time, the cross section for the p evaporation channel was deduced to be of the order of 0.1 nb [5] based on the observation of 1 fission event. In the present work, the same compound nucleus ^{259}Db* was chosen as the xn evaporation channels have lifetimes of the order of a second or more while the p and p2n evaporation channels lead to the unambiguous "fast" fission signal of ^{256,258}Rf with lifetimes under 20 ms. This letter shows that the cross-section measured at SHIP was overestimated and gives the first experimental measurement for pxn reaction cross sections leading to Rf nuclei at different bombarding energies. These results are compared to theoretical calculations and possible new avenues for synthesizing new heavy isotopes at the very top of the nuclear chart are also discussed.

2. Experimental details

The isotopes ^{256,257,258}Db were produced in ^{50}Ti(^{209}Bi, xn)$^{259-x}$Db reactions. The intense ^{50}Ti beam was provided by the U400 Cyclotron at the Flerov Laboratory of Nuclear Reactions in Dubna using the Metal Ions from Volatile Compounds (MIVOC) method [6]. The separator SHELS [7] was used to select the evaporation residues of interest and the newly upgraded GABRIELA detector array [8] was used to detect the residues and their subsequent α decay or fission as well as γ rays, X rays and conversion electrons. After selection in SHELS, the evaporation residues of interest pass through a Time of Flight (ToF) detector composed of 2 emissive foils and 4 large-size (70×90 mm^2) micro channel plate detectors. The residues are then implanted into a 10×10 cm^2 300 µm thick Double-sided Silicon Strip Detector (DSSD). With 128 strips on both sides, this DSSD provides 16384 individual pixels for position and time correlation of the implanted ion with subsequent decays. Particles escaping from the DSSD are detected in eight 6×5 cm^2 DSSDs with 16 strips on each side positioned upstream from the implantation detector and forming a tunnel. The Ge array consists of a large clover detector installed just behind the DSSD and 4 coaxial detectors forming a cross around the DSSD. All Ge detectors are equipped with BGO shields. Targets wheels accommodating 6 metallic Bi targets on a 3 µm Al backing were used. The average thickness of the Bi target segments on a given wheel varied from 0.38 to 0.51 mg/cm^2 $\pm$ 0.02 mg/cm^2. Calibrations of the DSSD were performed by implanting ^{209,210}Ra and ^{216,217}Th isotopes produced with ^{164}Dy and ^{170}Er targets respectively and observing their characteristic α decay. The calibration of the Ge detectors was performed using standard sources such as ^{152}Eu and ^{133}Ba, while the tunnel detectors were calibrated using the conversion electrons emitted in the decay of the 117 µs isomer in ^{209}Ra [9].

The data were taken in two experiments. The first experiment was performed in two campaigns. During the first campaign, cyclotron beam energies of 255 and 265 MeV were used, while in the second the primary beam energies were 255 and 275 MeV. Another difference between the two campaigns was the instrumentation of the DSSD. In the first instance, the amplification range on the DSSD allowed for the detection of internal conversion electrons and α particles, while in the second campaign, the amplification was changed to be able to measure α particles and fission up to $\sim$150 MeV. A fission event therefore leads to an overflow in the DSSD electronics channels during the first campaign and a high-energy signal above $\sim$40 MeV in the low-resolution amplification range of the DSSD during the second campaign. For the second experiment, primary beam energies of 255, 265 and 275 MeV were used and the amplification range of the DSSD electronics was also set to detect α particles and fission events.

The background conditions at the focal plane of SHELS, which depend mainly on the beam properties at the target position, are reflected in the ToF-detector counting rate. Data occurring at times where large background rates are recorded were discarded in the analysis.

An efficient true-fission tag is the coincident detection of at least one of the numerous photons emitted by the excited fission fragments. In the first experiment however, Compton-suppressed events were not recorded to disc while in the second experiment they were. This leads to very different efficiencies to detect the γ-ray flash accompanying a fission event: $\sim$25% in the first case and $\sim$90% in the others. Another way to distinguish fission events from background due to scattered beam is to require a coincident signal in the tunnel detectors as one of the fission fragments may escape the DSSD and be detected in one of the tunnel DSSDs and both fission fragments emit atomic electrons, which can also leave a signal in one of the tunnel detectors. Due to differences in electronics thresholds and the number of working channels in the tunnel detector, the efficiency for this tag is estimated to be $\sim$38% during the first experiment and $\sim$49% during the second experiment.

In the first experiment, the targets were covered with a 30 µg/cm^2 C coating on both sides to maximise heat evacuation by radiation and were rotated allowing currents of up to 300-350 pnA to be used. To quantify the possible contamination from ^{50}Ti-induced reactions on Pb impurities of the target, the experiment was repeated using Bi targets with a Pb impurity content of 0.1 10^{-5}%. These were not covered by a C coating.

3. Results

The neutron-evaporation residues of ^{259}Db were identified on the basis of known energies and lifetimes and mother-daughter correlation properties [11–13]. Fig. 1 shows the residue-α-α correlation plots obtained at 255 MeV and 265 MeV primary beam energies. Fission events were also observed and the distribution of fission times recorded at 255 MeV, 265 and 275 MeV primary beam energies are shown in Fig. 2. Fission events with a half-life of the order of a few seconds as well as fission events occurring less than 65 ms after the detection of an evaporation residue were observed, some of which were detected in coincidence with photons and/or conversion electrons and escape fission events in the tunnel detector. The "slow" fission events correspond to the fission of ^{258}Rf delayed by the unobserved electron capture (EC) of ^{258}Db and there may be a contribution from a spontaneous fission branch of ^{257}Db. Table 1 resumes the statistics collected regarding mother-daughter α-α correlations and Table 2 shows the information for "fast" fission events. The probability that the observed "fast" fission events stem from the tail of the longer-lived fission or background events has been estimated according to the prescription of reference [10]. The fact that 8 of the 22 observed fission events are found to be in coincidence with tunnel detectors, in drastically reduced background conditions, is further evidence that the events arise from the decay of short-lived states. Following the method

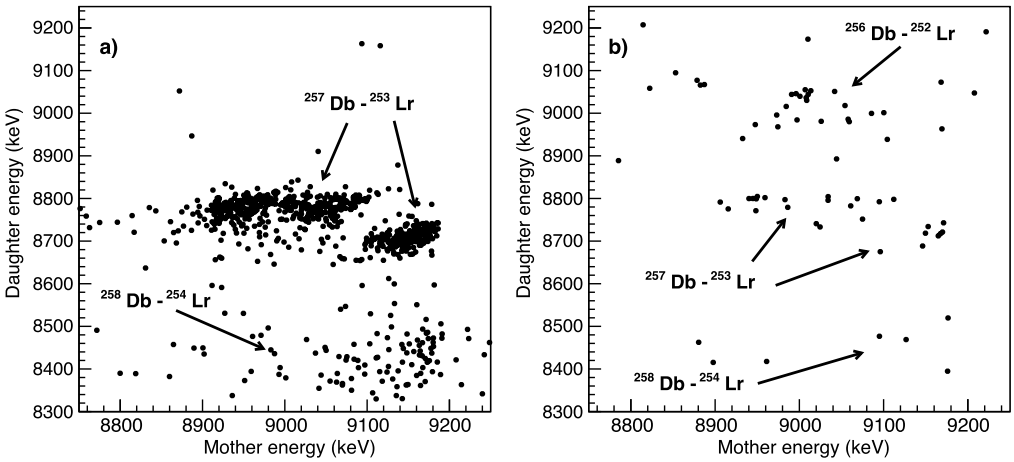

Fig. 1. a) Residue-mother-daughter correlations obtained for all the data taken at 255 MeV beam energy and b) for the data taken at 265 MeV. The energy limits used to extract the number of mother-daughter correlations of Table 1 are [8800-9200 keV] for $^{256-258}$Db mother decay energies and [8350-8600 keV], [8600-8850 keV] and [8850-9200 keV] for ^{254}Lr, ^{253}Lr and ^{252}Lr daughter decay energies respectively.

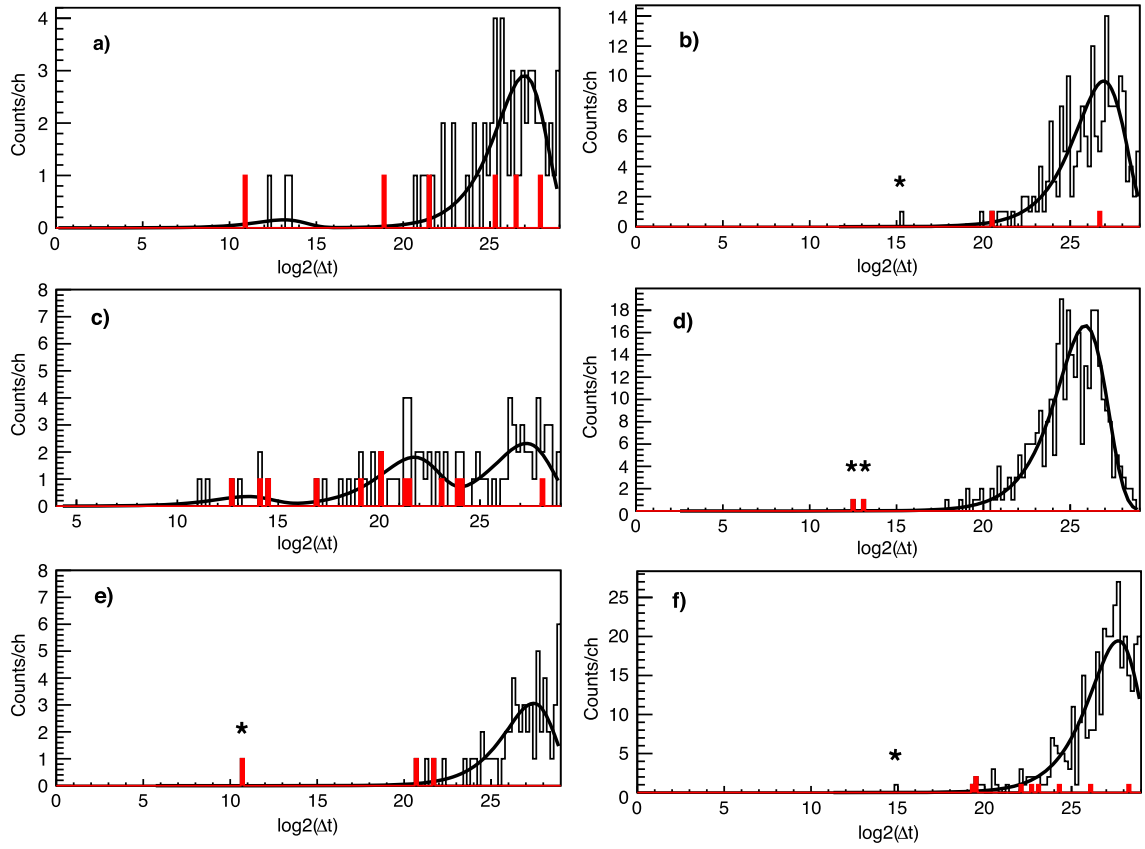

Fig. 2. Distribution of the time difference (in binary logarithm of the time difference Δt in μs) between recoil and fission events detected at the same position in the DSSD observed at a) 255 and b) 265 MeV in the 1st campaign of the 1st experiment, at c) 255 MeV and d) 275 MeV in the 2nd campaign of the first experiment and e-f) in 2 runs at 265 MeV during the 2nd experiment. In panel c) a 3-component fit to the time distribution of fission events is represented, where random events, "slow" and "fast" fission events clearly appear. The position Δt_{max} of each maxima gives the lifetime of the corresponding event: τ (μs) $= 2^{\Delta t_{max}}$ [17]. In panels a, b, d-f), the 1- or 2-component fits to the fission time distribution are also shown. The filled (red) histograms represent the fission events for which a coincidence with the backward tunnel detectors was recorded (see text for details). The "fast" fission events of interest are marked with an asterisk.

described in reference [10], the average half-lives of the "fast" fission events could be extracted and are also reported in Table 2. These values are consistent with the published spontaneous fission half-lives of ^{256}Rf (6.9(2) ms [14]) at the lowest and highest beam energies and with the literature values for the half-life of ^{258}Rf (10.0 ms [13,15] and 14.7 ms [16]) at the intermediate beam energy.

The nominal transmission and detection of SHELS for evaporation residues produced in fusion reactions with a ^{50}Ti beam is calculated to be 40% for xn and pxn channels. From the spatial distributions of the xn evaporation residues on the focal plane DSSD, the effective transmission and detection efficiency of evaporation residues was estimated to be 6.5(2.0)% and 28(5)% for the 2 campaigns in the first experiment and 23(5)% during the runs

Table 1
Number of residue-α-α correlations for the 1-, 2- and 3-neutron-evaporation channels obtained for every target wheel irradiated during the course of the 2 experiments. The average target-segment thickness on every target wheel, the mid-target beam energy and effective beam dose (i.e. in nominal background conditions) are also given.

E_b (MeV)	Bi target thickness (mg/cm^2)	E_{mid} (MeV)	Effective dose (particles)	1n	2n	3n
1st exp.	C-coated					
255	0.450	237.8	4.9 10^{17}	1	20	0
255	0.425	237.9	5.1 10^{17}	7	47	0
255	0.482	237.7	6.3 10^{17}	3	53	1
265	0.482	247.9	4.7 10^{17}	0	8	5
255	0.482	237.7	8.99 10^{17}	38	117	0
255	0.510	237.6	1.08 10^{18}	50	240	3
275	0.470	258.2	9.6 10^{17}	0	1	2
2nd exp.	not C-coated					
255	0.380	238.8	6.8 10^{17}	5	131	0
265	0.380	249.0	1.2 10^{18}	2	6	16
265	0.480	248.6	9.0 10^{17}	1	13	11
275	0.510	258.7	4.9 10^{17}	0	1	1

Table 2
Number of residue-fission correlations (with Δt(residue-fission)<65 ms) obtained for the different runs of the first and second experiments. The number of fission events recorded in coincidence with at least a Ge detector and a tunnel detector is indicated in parenthesis. The error probabilities that the events arise from the tail of the longer-lived fission events [10] are also reported together with the measured "fast" fission half-life $t_{1/2}$ and the resulting "fast" fission cross-sections σ_{ff}.

E_{mid} (MeV)	Fast fission events with (γ/tunnel)	Error Probability	$t_{1/2}$ (ms)	σ_{ff} (pb)
1st exp.				
237.8	3(0/1)	1.7 10^{-8}	5.9 $^{+8.1}_{-2.2}$	83 $^{+82}_{-39}$
237.9	0	-	-	$< 28\ ^{+66}_{-26}$
237.7	4(3/1)	7.9 10^{-16}	2.1 $^{+2.1}_{-0.7}$	80 $^{+68}_{-38}$
247.9	1(0/0)	5.6 10^{-2}	28 $^{+135}_{-13}$	27$^{+63}_{-24}$
237.7	3(0/0)	4.4 10^{-4}	2.7 $^{+3.6}_{-0.9}$	9 $^{+8}_{-3}$
237.6	7(2/3)	3.9 10^{-9}	7.6 $^{+4.6}_{-2.0}$	17 $^{+9}_{-5}$
258.2	2(2/2)	10^{-3}	5.0 $^{+12.1}_{-2.1}$	6$^{+8}_{-4}$
2nd exp.				
238.8	0	-	-	$< 6.6\ ^{+15.4}_{-5.8}$
249.0	1(1/1)	5.3 10^{-4}	1.1 $^{+5.3}_{-0.5}$	3.8 $^{+8.7}_{-3.3}$
248.6	1(1/0)	5.1 10^{-2}	21.5 $^{+103}_{-9.8}$	4.0 $^{+9.3}_{-3.5}$
258.7	0	-	-	$< 6.8\ ^{+15.9}_{-6.0}$

of the second experiment. The lower than expected transmissions are mainly due to the non optimal beam conditions on entering the separator. This in turn leads to different background conditions in the different runs. The recoil tagging efficiency was measured for each run by comparing the number of residue-α-α and α-α correlations and ranges from 87 to 93%. Using these efficiencies and assuming negligible EC and fission branches for ^{252,253}Lr and ^{257}Db isotopes and taking an EC branching ratio of 30% for the even Db isotopes and ^{254}Lr [18–21], the number of α-α correlations and fission events in Table 1 and Table 2 can be transformed into xn-evaporation and tentative pxn-evaporation cross sections. These are shown in Figs. 3 and 4 together with theoretical calculations.

The cross section for the synthesis of a superheavy nucleus in a heavy-ion fusion reaction with the subsequent emission of x neutrons and y protons can be calculated as

$$\sigma_{EvR}^{xn,yp}(E) = \frac{\pi\hbar^2}{2\mu E}\sum_{l=0}^{\infty}(2l+1)\,P_{\rm cont}(E,l)\times \quad (1)$$

$$\times\, P_{CN}(E,l)\cdot P_{xn,yp}(E,l)\,, \quad (2)$$

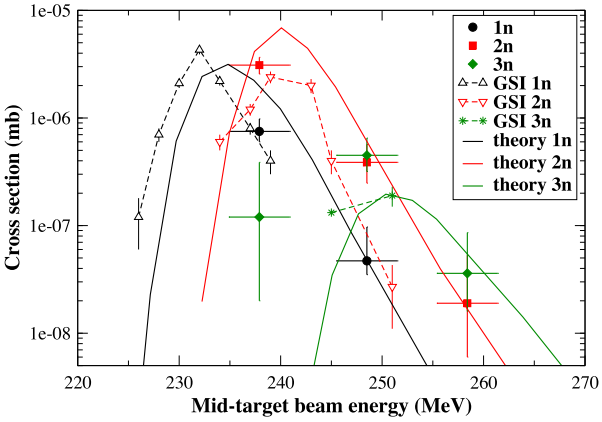

Fig. 3. Experimental cross sections for xn evaporation averaged over the first and second experiments as a function of mid-target beam energies. The mid-target beam energies have been obtained by correcting the cyclotron beam energies for energy losses in the C-coating (when present), the Al backing and half the target thicknesses. The errors account for a 1% uncertainty on the measurement of the beam energy as well as on the thickness of the Al backing. The dashed lines represent the measured cross sections at GSI [11] and the solid lines represent the theoretical 1, 2 and 3n neutron evaporation cross sections (see text for details).

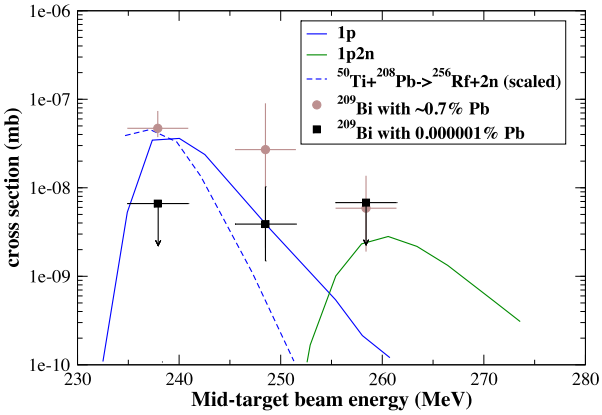

Fig. 4. Experimental and theoretical cross sections for pxn evaporation as a function of mid-target beam energies and target Bi enrichment. The solid lines are the result of theoretical calculations for the p and p2n evaporation channels and the dashed line is the scaled cross section for the ^{50}Ti(^{208}Pb, 2n) reaction (see text for details).

where μ is the reduced mass of the system, $P_{\rm cont}$ is the partial contact probability calculated within the channel coupling approach [22–25], P_{CN} is the probability of formation of a compound nucleus from the configuration of two touching nuclei [26] additionally adjusted to reproduce the data on the xn evaporation channels, and $P_{xn,yp}$ is the survival probability. We used the NRV statistical code of decay of excited nuclei [23–25] to obtain $P_{xn,yp}$. Within this model, the fission barriers are calculated as the difference between the liquid-drop barriers [27] and the shell corrections to the ground-state masses. The masses necessary for calculating the excitation energy of the compound nucleus, particle binding energies as well as the corresponding shell corrections are taken from Refs. [28,29].

The xn evaporation data presented in Fig. 3 are consistent with measurements performed at the velocity filter SHIP [11]. In Fig. 4, the excitation function for the production of ^{256}Rf via the ^{50}Ti(^{208}Pb, 2n) reaction [30] is also shown. It has been scaled according to the ^{208}Pb concentration measured in the Bi target used in the first experiment. X-ray fluorescence measurements on 3 samples of the targets give an estimate of 0.76(5)% for the Pb concentration. This in turn leads to a scaling factor of 0.36% when the natural abundance of ^{208}Pb is taken into account. It is directly

apparent from the comparison of the scaled 2n-evaporation cross section and the measured fission cross sections, that the ms fission events observed at the lowest beam energy during the first experiment can be attributed to the ^{208}Pb content of the target. This is not the case for the events observed at the other beam energies, which are reproduced with the pure Bi targets and must therefore arise from p evaporation of the ^{259}Db compound nucleus.

Based on the average lifetimes measured for the fission events at the intermediate and highest beam energies ($16.9^{+23.1}_{-6.2}$ ms and $5.0^{+12.1}_{-2.1}$ ms respectively), we assign the fission events observed at the intermediate energy to the p evaporation channel (^{258}Rf) and those observed at the highest beam energy to the p2n reaction channel (^{256}Rf). Nevertheless, a contribution from the p reaction cannot be excluded at the highest beam energy, given the present statistics and the fact that the lifetimes of ^{256}Rf and ^{258}Rf differ only by a factor of ∼2. On the basis of these assignments, the data suggests that the order of magnitude for the ratio between theoretical xn and p and p2n reaction cross sections is correct. The p1n evaporation channel cannot be investigated as it relies on determining correctly the number of ^{257}Rf-^{253}No correlations stemming from ^{257}Rf produced directly in the fusion-evaporation reaction. These rare correlations however, cannot be unambiguously distinguished from those following the EC of ^{257}Db or from ^{258}Rf-^{254}No correlations following the EC of ^{258}Db.

4. Conclusion and outlook

The present measurement gives the first experimental values for the cross section of fusion and pxn evaporation leading to a super heavy nucleus. Due to the limited statistics and number of data points, the exact shapes and positions of the p and p2n excitation functions could, however, not be determined. This would have given insight into the magnitude of the Coulomb barrier for proton emission, which is sensitive to the shape of the emitting nuclear system. More data on the competition between neutron and proton evaporation is needed to constrain and improve the theoretical reaction models, which suffer from many uncertainties and have therefore a limited accuracy [31]. This can be done via decay spectroscopy when the decay properties of the pxn residue are clearly different to the ones of any xn residue and especially if one can distinguish direct production of the nucleus of interest with respect to indirect production via EC of an xn channel. Another alternative is to perform decay spectroscopy of mass-identified residues using a recoil separator with sufficient mass resolution, such as is expected at S3 in GANIL/SPIRAL2 [32] for example, or for long-enough lifetimes, at the focal plane of mass-sensitive devices such as MASHA in Dubna [33] or FIONA in Berkeley [34]. Such studies should greatly benefit from the availability of more intense beams at accelerator facilities around the world, such as the future Super Heavy Element Factory in Dubna [35].

The results presented in this paper are encouraging for future production of new, more neutron rich superheavy isotopes. Indeed, recent calculations of proton-emission channels leading to isotopes of $Z = 111$-117 give cross sections of p-emission channels that are 30-100 times smaller than the n-evaporation channels [36]. The use of high beam intensities, combined with efficient experimental setups should therefore allow to access and study nuclei closer to the centre of the Island of Stability. At lower mass, the synthesis and spectroscopy of new more neutron rich isotopes, which cannot be reached by neutron-evaporation channels using available targets and projectiles, may become possible.

Acknowledgements

The authors would like to acknowledge the role of Y. Ts. Oganessian in this work and thank him for the suggestion to investigate the production of heavy isotopes via the evaporation of charged particles. This work was supported by the Russian Foundation for Basic Research (projects nos. 18-52-15004 and 17-02-00867), the French National Research Agency (projects nos. ANR-06-BLAN-0034-01 and ANR-12-BS05-0013) and the IN2P3-JINR collaboration agreement no. 04-63. One of us (D. Ackermann) is supported by the European Commission in the framework of CEA-EUROTALENT 2014-2018 (no PCOFUND – GA – 2013 - 600382).

References

[1] Y.T. Oganessian, V.K. Utyonkov, Super-heavy element research, Rep. Prog. Phys. 78 (3) (2015) 036301, http://stacks.iop.org/0034-4885/78/i=3/a=036301.
[2] V.I. Zagrebaev, A.V. Karpov, W. Greiner, Possibilities for synthesis of new isotopes of superheavy elements in fusion reactions, Phys. Rev. C 85 (2012) 014608, https://doi.org/10.1103/PhysRevC.85.014608, https://link.aps.org/doi/10.1103/PhysRevC.85.014608.
[3] V. Druin, Book of abstracts of the international school-seminar on heavy ion physics, in: JINR (Ed.), Alushta, Crimea, 1983, Dubna, Moscow Region.
[4] Y.T. Oganessian, Radiochim. Acta 37 (1984) 113.
[5] F.P. Heßberger, G. Mü nzenberg, S. Hofmann, Y.K. Agarwal, K. Poppensieker, W. Reisdorf, K.H. Schmidt, J.R.H. Schneider, W.F.W. Schneider, H.J. Schö tt, P. Armbruster, B. Thuma, C.C. Sahm, D. Vermeulen, The new isotopes ^{258}105, ^{257}105, ^{254}Lr and ^{253}Lr, Z. Phys. A 322 (1985) 557.
[6] J. Rubert, J. Piot, Z. Asfari, B. Gall, J. Ärje, O. Dorvaux, P. Greenlees, H. Koivisto, A. Ouadi, R. Seppälä, First intense isotopic titanium-50 beam using MIVOC method, Nucl. Instrum. Methods Phys. Res., Sect. B, Beam Interact. Mater. Atoms 276 (2012) 33, https://doi.org/10.1016/j.nimb.2012.01.028, http://www.sciencedirect.com/science/article/pii/S0168583X12000511.
[7] A.V. Yeremin, A. Popeko, O.N. Malyshev, A. Lopez-Martens, K. Hauschild, O. Dorvaux, B. Gall, V. Chepigin, A.I. Svirikhin, A. Isaev, E.A. Sokol, M.L. Chelnokov, A.N. Kuznetsov, A.A. Kusznetsova, A.V. Belozerov, K. Rezynkina, F. Dechery, F. Le Blanc, J. Piot, J. Gehlot, D. Tonev, E. Stefanova, D. Pantelika, C. Nita, B. Andel, S. Mulins, P. Jones, S. Ntshangase, Phys. Part. Nucl. Lett. 12 (2015) 35.
[8] K. Hauschild, A. Yeremin, O. Dorvaux, A. Lopez-Martens, A. Belozerov, C.B. on, M. Chelnokov, V. Chepigin, S. Garcia-Santamaria, V. Gorshkov, F. Hanappe, A. Kabachenko, A. Korichi, O. Malyshev, Y. Oganessian, A. Popeko, N. Rowley, A. Shutov, L. Stuttgé, A. Svirikhin Gabriela, A new detector array for γ-ray and conversion electron spectroscopy of transfermium elements, Nucl. Instrum. Methods Phys. Res., Sect. A, Accel. Spectrom. Detect. Assoc. Equip. 560 (2) (2006) 388–394, https://doi.org/10.1016/j.nima.2006.01.107, http://www.sciencedirect.com/science/article/pii/S0168900206001069.
[9] K. Hauschild, A. Lopez-Martens, A.V. Yeremin, O. Dorvaux, A.V. Belozerov, M.L. Chelnokov, V.I. Chepigin, B. Gall, V.A. Gorshkov, M. Guttormsen, P. Jones, A.P. Kabachenko, A. Khouaja, A.C. Larsen, O.N. Malyshev, A. Minkova, H.T. Nyhus, Y.T. Oganessian, D. Pantelica, A.G. Popeko, F. Rotaru, S. Saro, A.V. Shutov, S. Siem, A.I. Svirikhin, N.U.H. Syed, Half-life and excitation energy of the $i^{\pi}=13/2^{+}$ isomer in ^{209}Ra, Phys. Rev. C 77 (2008) 047305, https://doi.org/10.1103/PhysRevC.77.047305, https://link.aps.org/doi/10.1103/PhysRevC.77.047305.
[10] K.H. Schmidt, C.C. Sahm, K. Pielenz, H.G. Clerc, Some remarks on the error analysis in the case of poor statistics, Z. Phys. A 316 (1) (1984) 19–26, https://doi.org/10.1007/BF01415656.
[11] F. Heßberger, S. Hofmann, D. Ackermann, V. Ninov, M. Leino, G. Münzenberg, S. Saro, A. Lavrentev, A. Popeko, A. Yeremin, C. Stodel, Decay properties of neutron-deficient isotopes ^{256,257}Db, ^{255}Rf, ^{252,253}Lr, Eur. Phys. J. A 12 (1) (2001) 57–67, https://doi.org/10.1007/s100500170039.
[12] F.P. Heßberger, S. Hofmann, B. Streicher, B. Sulignano, S. Antalic, D. Ackermann, S. Heinz, B. Kindler, I. Kojouharov, P. Kuusiniemi, M. Leino, B. Lommel, R. Mann, A.G. Popeko, Š. Šáro, J. Uusitalo, A.V. Yeremin, Decay properties of neutron-deficient isotopes of elements from $Z = 101$ to $Z = 108$, Eur. Phys. J. A 41 (2) (2009) 145–153, https://doi.org/10.1140/epja/i2009-10826-2.
[13] F.P. Heßberger, S. Antalic, D. Ackermann, B. Andel, M. Block, Z. Kalaninova, B. Kindler, I. Kojouharov, M. Laatiaoui, B. Lommel, A.K. Mistry, J. Piot, M. Vostinar, Investigation of electron capture decay of 258Db and α decay of 258Rf, Eur. Phys. J. A 52 (11) (2016) 328, https://doi.org/10.1140/epja/i2016-16328-2.
[14] P.T. Greenlees, J. Rubert, J. Piot, B.J.P. Gall, L.L. Andersson, M. Asai, Z. Asfari, D.M. Cox, F. Dechery, O. Dorvaux, T. Grahn, K. Hauschild, G. Henning, A. Herzan, R.-D. Herzberg, F.P. Heßberger, U. Jakobsson, P. Jones, R. Julin, S. Juutinen, S. Ketelhut, T.-L. Khoo, M. Leino, J. Ljungvall, A. Lopez-Martens, R. Lozeva, P. Nieminen, J. Pakarinen, P. Papadakis, E. Parr, P. Peura, P. Rahkila, S. Rinta-Antila, P. Ruotsalainen, M. Sandzelius, J. Sarén, C. Scholey, D. Seweryniak, J. Sorri, B. Sulignano, C. Theisen, J. Uusitalo, M. Venhart, Shell-structure and pairing interaction

in superheavy nuclei: Rotational properties of the Z = 104 nucleus ^{256}Rf, Phys. Rev. Lett. 109 (2012) 012501, https://doi.org/10.1103/PhysRevLett.109.012501, https://link.aps.org/doi/10.1103/PhysRevLett.109.012501.

[15] F.P. Heßberger, Spontaneous fission properties of superheavy elements, Eur. Phys. J. A 53 (4) (2017) 75, https://doi.org/10.1140/epja/i2017-12260-3.

[16] J.M. Gates, M.A. Garcia, K.E. Gregorich, C.E. Düllmann, I. Dragojević, J. Dvorak, R. Eichler, C.M. Folden, W. Loveland, S.L. Nelson, G.K. Pang, L. Stavsetra, R. Sudowe, A. Türler, H. Nitsche, Synthesis of rutherfordium isotopes in the ^{238}U(^{26}Mg, xn)$^{264-x}$Rf reaction and study of their decay properties, Phys. Rev. C 77 (2008) 034603, https://doi.org/10.1103/PhysRevC.77.034603, https://link.aps.org/doi/10.1103/PhysRevC.77.034603.

[17] A. Lopez-Martens, K. Hauschild, A.V. Yeremin, O. Dorvaux, A.V. Belozerov, C. Briançon, M.L. Chelnokov, V.I. Chepigin, D. Curien, P. Désesquelles, B. Gall, V.A. Gorshkov, M. Guttormsen, F. Hanappe, A.P. Kabachenko, F. Khalfallah, A. Korichi, A.C. Larsen, O.N. Malyshev, A. Minkova, Y.T. Oganessian, A.G. Popeko, M. Rousseau, N. Rowley, R.N. Sagaidak, S. Sharo, A.V. Shutov, S. Siem, L. Stuttgé, A.I. Svirikhin, N.U.H. Syed, C. Theisen, Isomeric states in 253No, Eur. Phys. J. A 32 (3) (2007) 245–250, https://doi.org/10.1140/epja/i2007-10391-8.

[18] Y. Akovali, Nuclear data sheets for A = 250, 254, 258, 262, 266, Nucl. Data Sheets 94 (1) (2001) 131–225, https://doi.org/10.1006/ndsh.2001.0018, http://www.sciencedirect.com/science/article/pii/S0090375201900183.

[19] B. Singh, Nuclear data sheets for A = 256, Nucl. Data Sheets 141 (2017) 327–364, https://doi.org/10.1016/j.nds.2017.03.002, http://www.sciencedirect.com/science/article/pii/S0090375217300261.

[20] E. Browne, J. Tuli, Nucl. Data Sheets 114 (8) (2013) 1041–1185, https://doi.org/10.1016/j.nds.2013.08.002, http://www.sciencedirect.com/science/article/pii/S0090375213000549.

[21] A. Bhagwat, N. Thompson, J. Tuli, Nuclear data sheets for A = 254, Nucl. Data Sheets 105 (4) (2005) 959–986, https://doi.org/10.1016/j.nds.2005.10.002, http://www.sciencedirect.com/science/article/pii/S0090375205000591.

[22] V. Zagrebaev, V. Samarin, Phys. At. Nucl. Lett. 67 (2004) 1462.

[23] V. Zagrebaev, A. Denikin, A. Karpov, A. Alekseev, M. Naumenko, V. Rachkov, V. Samarin, V. Saiko, NRV web knowledge base on low-energy nuclear physics, http://nrv.jinr.ru.

[24] A.V. Karpov, A.S. Denikin, A.P. Alekseev, V.I. Zagrebaev, V.A. Rachkov, M. Naumenko, V.V. Saiko, Phys. At. Nucl. 79 (2016) 749.

[25] A. Karpov, A. Denikin, M. Naumenko, A. Alekseev, V. Rachkov, V. Samarin, V. Saiko, V. Zagrebaev, NRV web knowledge base on low-energy nuclear physics, Nucl. Instrum. Methods Phys. Res., Sect. A, Accel. Spectrom. Detect. Assoc. Equip. 859 (2017) 112–124, https://doi.org/10.1016/j.nima.2017.01.069, http://www.sciencedirect.com/science/article/pii/S0168900217301584.

[26] V. Zagrebaev, W. Greiner, Synthesis of superheavy nuclei: a search for new production reactions, Phys. Rev. C 78 (2008) 034610, https://doi.org/10.1103/PhysRevC.78.034610, https://link.aps.org/doi/10.1103/PhysRevC.78.034610.

[27] A.J. Sierk, Macroscopic model of rotating nuclei, Phys. Rev. C 33 (1986) 2039–2053, https://doi.org/10.1103/PhysRevC.33.2039, https://link.aps.org/doi/10.1103/PhysRevC.33.2039.

[28] M. Wang, G. Audi, A. Wapstra, F. Kondev, M. MacCormick, X. Xu, B. Pfeiffer, The Ame2012 atomic mass evaluation, Chin. Phys. C 36 (12) (2012) 1603, http://stacks.iop.org/1674-1137/36/i=12/a=003.

[29] P. Möller, A. Sierk, T. Ichikawa, H. Sagawa, Nuclear ground-state masses and deformations: FRDM (2012), At. Data Nucl. Data Tables 109–110 (2012) 1–204, https://doi.org/10.1016/j.adt.2015.10.002, http://www.sciencedirect.com/science/article/pii/S0092640X1600005X, 2016.

[30] S. Hofmann, Properties of heavy nuclei measured at the GSI SHIP, Nucl. Phys. A 734 (2004) 93–100, https://doi.org/10.1016/j.nuclphysa.2004.01.018, http://www.sciencedirect.com/science/article/pii/S0375947404000235.

[31] V.I. Zagrebaev, Y. Aritomo, M.G. Itkis, Y.T. Oganessian, M. Ohta, Synthesis of superheavy nuclei: how accurately can we describe it and calculate the cross sections?, Phys. Rev. C 65 (2001) 014607, https://doi.org/10.1103/PhysRevC.65.014607, https://link.aps.org/doi/10.1103/PhysRevC.65.014607.

[32] A. Drouart, J.A. Nolen, H. Savajols, Super separator spectrometer for the LINAG heavy ion beams, Int. J. Mod. Phys. E 18 (10) (2009) 2160–2168, https://doi.org/10.1142/S0218301309014482.

[33] A.M. Rodin, A.V. Belozerov, D.V. Vanin, V.Y. Vedeneyev, A.V. Gulyaev, A.V. Gulyaeva, S.N. Dmitriev, M.G. Itkis, J. Kliman, N.A. Kondratiev, L. Krupa, Y.T. Oganessian, V.S. Salamatin, I. Siváček, S.V. Stepantsov, E.V. Chernysheva, S.A. Yuchimchuk, MASHA separator on the heavy ion beam for determining masses and nuclear physical properties of isotopes of heavy and superheavy elements, Instrum. Exp. Tech. 57 (4) (2014) 386–393, https://doi.org/10.1134/S0020441214030208.

[34] J.M. Gates, G.K. Pang, J.L. Pore, K.E. Gregorich, J.T. Kwarsick, G. Savard, N.E. Esker, M. Kireeff Covo, M.J. Mogannam, J.C. Batchelder, D.L. Bleuel, R.M. Clark, H.L. Crawford, P. Fallon, K.K. Hubbard, A.M. Hurst, I.T. Kolaja, A.O. Macchiavelli, C. Morse, R. Orford, L. Phair, M.A. Stoyer, First direct measurements of superheavy-element mass numbers, Phys. Rev. Lett. 121 (2018) 222501, https://doi.org/10.1103/PhysRevLett.121.222501, https://link.aps.org/doi/10.1103/PhysRevLett.121.222501.

[35] S. Dmitriev, M. Itkis, Y. Oganessian, Status and perspectives of the Dubna Superheavy Element Factory, EPJ Web Conf. 131 (2016) 08001, https://doi.org/10.1051/epjconf/201613108001.

[36] J. Hong, G. Adamian, N. Antonenko, Ways to produce new superheavy isotopes with Z = 111−117 in charged particle evaporation channels, Phys. Lett. B 764 (2017) 42–48, https://doi.org/10.1016/j.physletb.2016.11.002, http://www.sciencedirect.com/science/article/pii/S0370269316306633.